CHARACTERIZATION OF PURE MODE I, II AND III DELAMINATION OF LAMINATED COMPOSITE BY USING EDGE RING CRACK SPECIMEN

Yangyang Ge[1], Xiaojing Gong*[1], Emmanuel De Luycker[1], Anita Hurez[2],
[1] Institut Clément Ader, CNRS UMR 5312, Université de Toulouse, UPS, France
Email: xiaojing.gong@iut-tarbes.fr
[2] DRIVE EA1859, Univ. Bourgogne Franche Comte, F58000, Nevers France

Keywords: Testing method, Pure mode I delamination, Pure mode II delamination, Pure mode III delamination, Edge Ring Crack (ERC) specimen

ABSTRACT

Edge Ring Crack (ERC) specimen tests are proposed in order to study pure mode I, mode II and mode III delamination behavior of laminated composite. Two experimental devices were designed and realized. The same device can be used for mode I and mode III delamination tests. Virtual crack closure technique in finite element analysis was performed to determine the distribution of strain energy release rate along the crack tip. It demonstrates that the participation of unwanted fracture modes can be eliminated in order to obtain a pure mode delamination by using the ERC specimens. Moreover, the evolution of strain energy release rate along the crack tip is proved to be quite uniform for a given fracture mode. Thus the toughness under three pure modes have been determined on a woven carbon/epoxy composite made from a taffeta fabric prepreg and the results obtained are very closed to those measured by well-known delamination tests.

1.Introduction

Delamination is one of the most common and dangerous damage modes in a laminated composite, which generally occurs under mixed mode loading conditions. The criterion of delamination toughness under mixed mode I+II+III is not yet satisfactory because the investigation of mode III component is quite limited. The determination of the mode III delamination critical strain energy release rate, G_{IIIC}, of laminated polymeric matrix composite materials has proven to be a complex issue.

In fact, even pure mode III delamination test is not simple to achieve, because it is neither easy to eliminate completely the mode I and mode II components nor to obtain a uniform value of mode III strain energy release rate (G_{III}) along the crack tip. In experimental tests, an average value of G_{III} along the crack tip is generally considered in the determination of G_{IIIC} by a closed-form expression, so high variation of G_{III} along the crack tip would cause excessive error in the measurement of G_{IIIC}. Unfortunately, in most existing tests such as Crack Rail Shear test[1], Split Cantilever Beam test[2] and Edge Crack Torsion test[3], a slight evolution of G_{III} along the crack tip can be observed in the central region of the crack tip and more significant one at the extremities. The later one is due to the free edge effects. Moreover, mode II component can never be totally eliminated in most cases.

In this study, a specimen with a circular crack tip called Edge Ring Crack (ERC) specimen was tested. The main advantage of this shape is the total absence edge and so edge effects on the results. With the help of different test devices, different loading modes can be introduced so that the behavior of laminated composites under every pure mode delamination, even under some mixed mode ones can be investigated.

In our previous work, an Edge Ring Crack Torsion (ERCT)[4] test has been realized for the characterization of pure mode III delamination. This work focuses on further improvement of pure mode III delamination by updating ERCT device. Furthermore the ERC specimens are also tested under pure mode I and pure mode II loads.

2.Experimental

2.1.Materials and specimens

In this research work, all ERC specimens were obtained from a woven carbon/epoxy taffeta fabric prepreg (ref: IMP503Z). The properties of the prepreg are listed in Table 1.

Table 1. Properties of the prepreg used in the tested laminates

Fabric weight	200 (g/m^2)
Glass transition temperature T_g	120 (°C)
Percentage of matrix V_m	42%
Longitudinal and transverse modulus: E_{11}=E_{22}	55250 (MPa)
Out-of-plane shear modulus G_{13}=G_{23}	5400(MPa)
Tensile strength in direction 1 and 2: X^+= Y^+	669 (MPa)
Poisson's ratio 12: ν_{12}	0,044
Shear modulus in direction 12: G_{12}	4062 (MPa)
Shear strength in direction 12: S_{12}	117 (MPa)

The composite laminate was manufactured by hand lay-up technique and a 13 µm thick polyester film was inserted in the midplane in order to create a pre-crack. 32 plies were used for the whole laminate and the stacking sequence is [0/45/45/0/45/0/0/45/45/0/0/45/0/45/45/0]//crack//[0/45/45/0/45/0/0/45/45/0/0/45/0/45/45/0], where 0 represents a taffeta balanced fabric ply with yarns oriented in 0° and 90° while 45 represents the same fabric oriented in ±45°. The laminate is symmetric with respect to the pre-crack.

ERC specimen is shown in Figure 1. A pre-crack with a circular front is created between two sub-laminates by inserting a 13 µm thick polyester film during the manufacturing process. A disc is cut out in the center of the polyester film with the help of a circle cutter. In order to locate the center of the circular hole on the rotation axes of the machine, the center of the hole is identified on the outer skins of the sample. The precise location of the hole has been verified by Ultrasonic C-scan. The geometry of ERC specimen is: diameter of the disc d=50mm, sides length D=120mm, and thickness h=7mm.

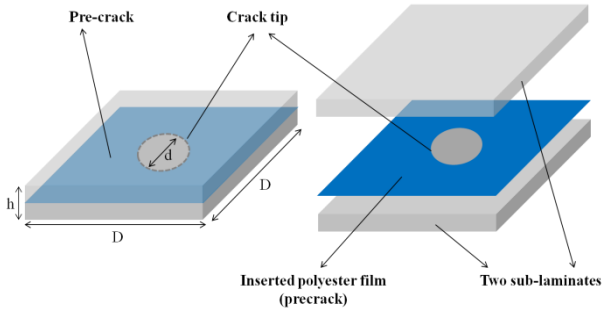

Figure 1. Edge Ring Crack (ERC) specimen

2.2.Development of experimental devices

The ERCT test device is shown in

Figure ***2***. Firstly, the composite specimen is pasted to the ring protruding from two rigid plates. Great care should be taken in order to locate the center of the hole in the sample on the axes of the rigid plate during the gluing process. Secondly the rigid plates are screwed to the torsion devise. Finally, the torsion devise is submitted to an imposed rotation up to the propagation of the crack. Thanks to the holes in the rigid plates, it's also possible to observe the crack propagation by Ultrasonic C-scan. A delamination in pure mode III occurs with a fairly uniform evolution of G_{III} along the crack tip of the specimen.

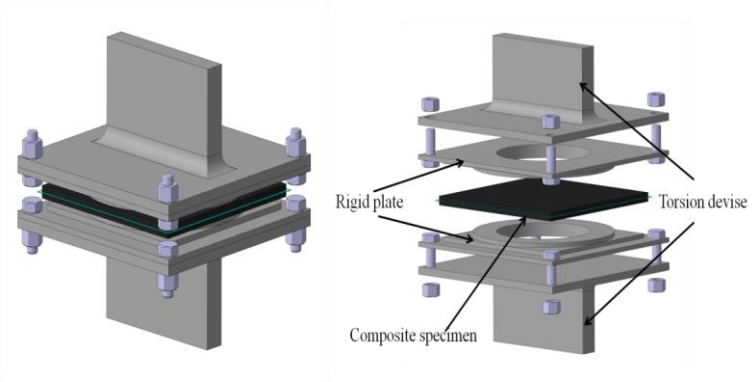

Figure 2. Edge Ring Crack Torsion test device

In the present work, the original ERCT device has been updated Figure 3(c) aiming at further improvements mainly on the evolution of G_{III} along the crack tip. The main modification lies on the symmetry of the torsion device that has been improved in order to match the axisymmetrical loading condition. The dimension of the ring protruding is maintained with an inner and outer diameter of 80mm and 120mm. Moreover, the pure mode I and the pure mode II load can be introduced on the same ERC specimen. The former one uses the same device as the one used for mode III test while a new device is proposed for the later one, shown in Figure 3(a) and (b). Note that ERC specimens are pasted to the devices in mode I and mode III delamination tests. The pictures of the three tests are shown in Figure 4. In this way, the three pure modes toughness measured should be more representatives without any more additional effects dues to geometry change on the results. Note that there is little difference between a circular and a square ERC specimen when their diameter and length are equal. In this work square ERC specimens were employed.

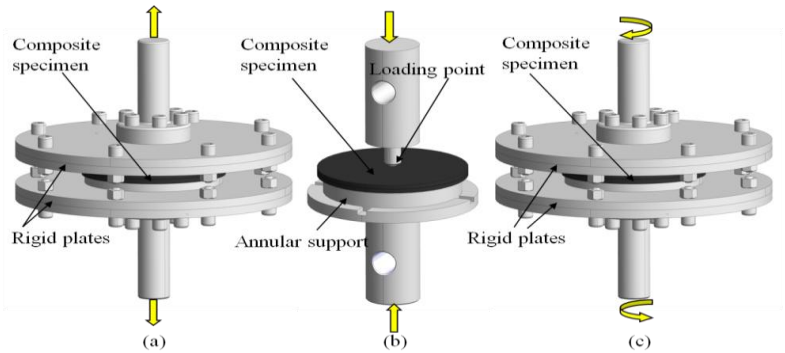

Figure 3. Devices for pure mode I (a), pure mode II (b) and pure mode III (c)

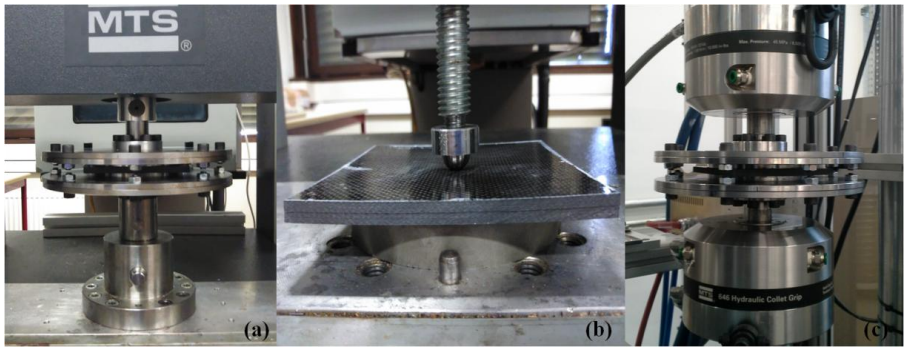

Figure 4. (a) ERC-I test; (b) ERC-II test; (c) ERC- III test

2.3.Testing methods

All the tests were carried out at ambient temperature. An axial rotation speed of 0.5°/min was imposed for mode III delamination test. An axial displacement speed of 2mm/min was imposed for mode I and mode II delamination tests.

Figure 4(a) shows ERC-I device mounted on the tensile machine. Firstly, the composite specimen was pasted to the ring protruding from the two rigid plates. Secondly the rigid plates were screwed to the tensile devise. Finally, the tensile device was submitted to an imposed traction up to the propagation of the crack.
Figure 4(b) shows ERC-II device placed under compression. The specimen was put on a rigid supporting ring and then loaded in the centre of the specimen. Attention was paid to keep coincidence of the centers of loading point, the specimen and the ring.
Figure 4(c) shows ERC-III device mounted on the torsion machine. Firstly, the composite specimen was pasted to the ring protruding from the two rigid plates. Secondly the rigid plates were screwed to the torsion devise; great care was paid before the screws were secured in order to ensure the coaxiality of the specimen with the machine. Finally, the torsion devise was submitted to an imposed rotation up to the propagation of the crack.

3.Finite element analysis

In this work, numerical modeling was performed using Ls-Dyna finite element software. The fixtures and specimens were modeled by 3D solid elements. Spring elements were located along the crack tip

in order to obtain loads at the crack tip. MAT 22 was chosen to simulate the composite laminates due to its better performance, where geometry nonlinear shear behavior and Changchang fracture criterion for orthotropic materials have been adopted. Then the virtual crack closure technique (VCCT)[5;6] is performed to determine the evolution of G_I, G_{II} and G_{III} along the crack tip. Contact_automatic_surface_to surface was applied on the two delamination surfaces to prevent interpenetration during the analysis. Relative sliding between points within the delamination plane is assumed to be frictionless.

Every ply was set up independently according to the stacking sequence. One element was set in the thickness of each ply. The principal mechanical properties of material were set according to Table 1. The mesh along the crack tip was specially refined to guarantee the model convergence. For example, the mesh used for ERC-II modelisation is shown in

Figure ***5***. Besides, meshes for ERC-I and ERC-III tests models are shown in

Figure ***6***.

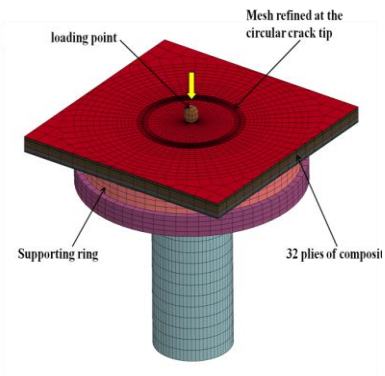

Figure 5. Mesh for ERC-II

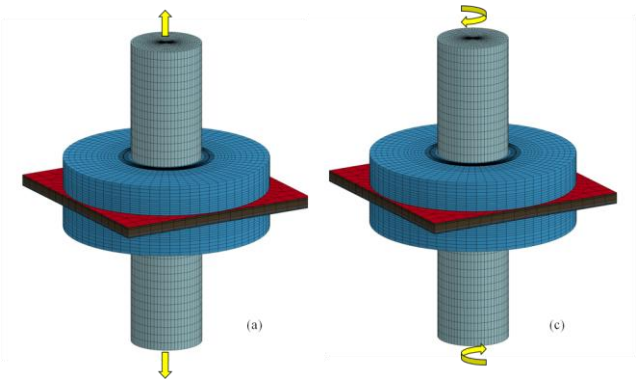

Figure 6. Mesh for ERC-I (a) and ERC-III (b)

4.Results and discussion

4.1.Edge Ring Crack Torsion (ERCT) test or Edge Ring Crack mode III test (ERC-III)

In the ERC-III test, the crack propagates towards the centre in an unstable manner. Figure 7 shows a typical experimental torque/rotation angle curve, where a sudden drop in the torque is observed. Herein, the repeatability with specimens is relatively good. The peak load is almost at the end of the linear part. That results in an easy definition of the critical load corresponding to the crack growth onset.

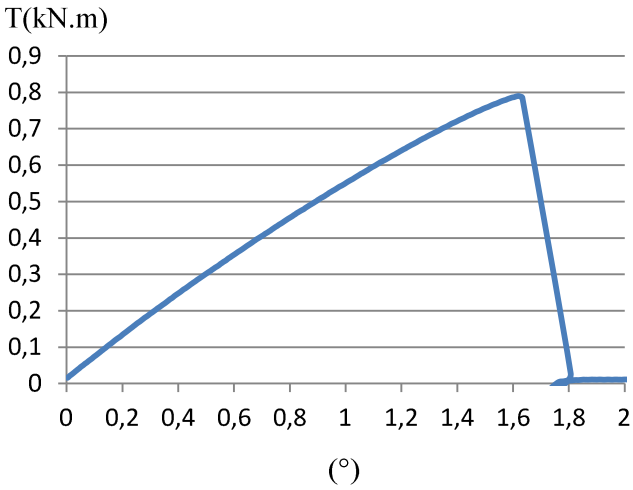

Figure 7. Typical experimental torque/rotation angle curve

A finite element model was established and VCCT was performed to determine G_{IIIC}. Figure 8 shows that the distribution of G_{III} along the crack tip, using the modified device, is more uniform than the one with the original device and that the standard deviation relative to the average value is less than 1.9%. As a comparison the standard deviation relative to the average value of G_{III} can be nearly 22% in our previous ECT test because the value of G_{III} drops to nearly 0 at the extremities of the crack tip. Moreover, mode I and mode II components stays below 1.4% and can be considered as negligible in this test as shown in Figure 9. For ECT test, mode II component becomes principal mode at the extremities of the crack tip. In conclusion, a pure mode III delamination test with uniform distribution of G_{III} along the crack tip is achieved. Therefore, the average value is defined as G_{IIIC}. With the average critical load of a series of tests, the value of G_{IIIC} is given as 1139(N/m), which is reasonable compared to 750(N/m) in ENF test .

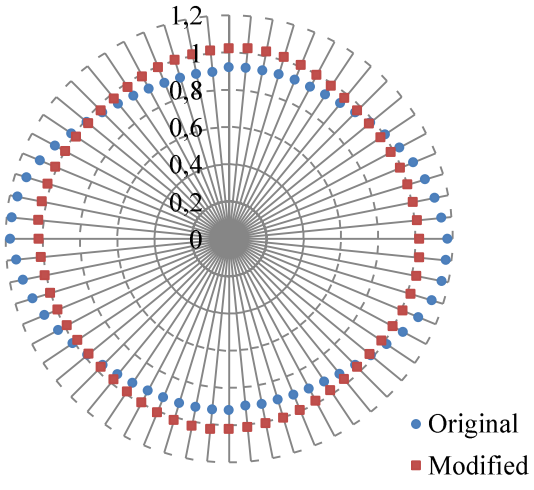

Figure 8. Evolution of normalized G_{III} along the circular crack tip with original and new ERC-III devices

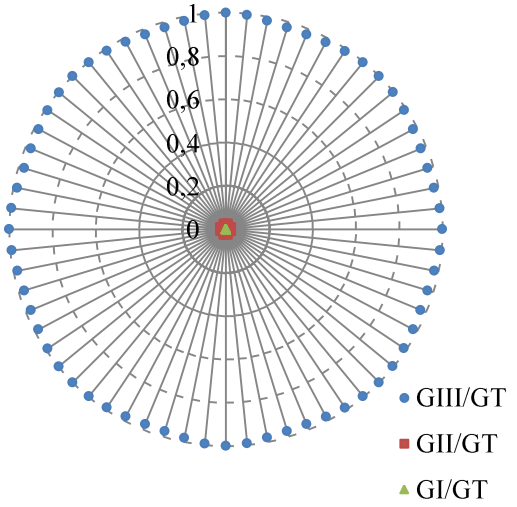

Figure 9. Evolution of normalized G_I, G_{II}, G_{III} along the circular crack tip with new ERC-III device

4.2.Edge Ring Crack mode II test (ERC-II)

Figure ***10*** shows a typical experimental force-displacement curve, where a sudden drop in the compression is observed. Most of the advantages of ERC-III are kept in the mode II test. A finite element model was established and the VCCT was performed to determine G_{IIC}. Figure 11 shows the distribution of G_I, G_{II} and G_{III} along the crack tip. The distribution of G_{II} along the crack tip is uniform with approximately 1.2% standard deviation relative to the average value. Moreover, the mode I and mode III components are less than 1.8% and can be considered as negligible. As a comparison, the standard deviation is approximately 14% in our previous End Notch Flexion (ENF) test. In conclusion, a pure mode II delamination test with uniform distribution of G_{II} along the crack tip is achieved. Therefore, the average value of G_{II} from the VCCT at a the critical load is defined as G_{IIC}. With the average critical load of a series tests, the value of G_{IIC} is given as 1121(N/m), which is reasonable compared to 1213(N/m) in ENF test.

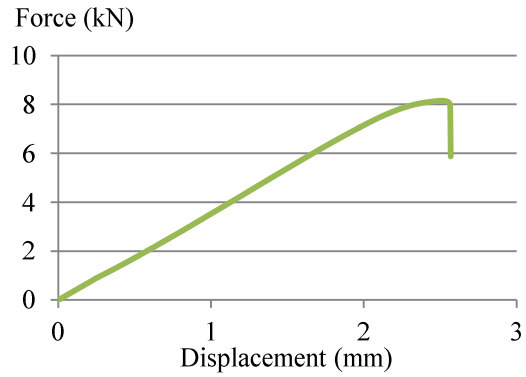

Figure 10. Typical experimental force/displacement curve

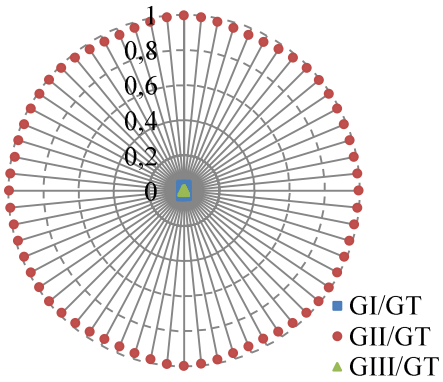

Figure 11. Evolution of normalized G_I, G_{II}, G_{III} along the circular crack tip in ERC-I test

4.3.Edge Ring Crack-I(ERC-I) test

Typical experimental force/displacement curve is shown in Figure 12. A finite element model was established and the VCCT was performed to determine G_{IC}. Figure 13 shows the distribution of G_I, G_{II} and G_{III} along the crack tip in ERC-I test. The distribution of G_I along the crack tip was uniform with approximately 0.04% standard deviation relative to the average value. Moreover, the mode II and mode III components are less than 0.05% and can be considered as negligible. As a comparison, the standard deviation is approximately 32% in our previous Double Cantilever Beam test and mode II component becomes the principal mode at the extremities of the crack tip. In conclusion, a pure mode I delamination test with uniform distribution of G_I along the crack tip is achieved. Therefore, the average value is defined as the toughness G_{IC}. With the average critical load on a set of samples, namely the maximum tensile load, the value of G_{IC} is given as 305N/m, which is reasonable compared to 330(N/m) in ENF test .

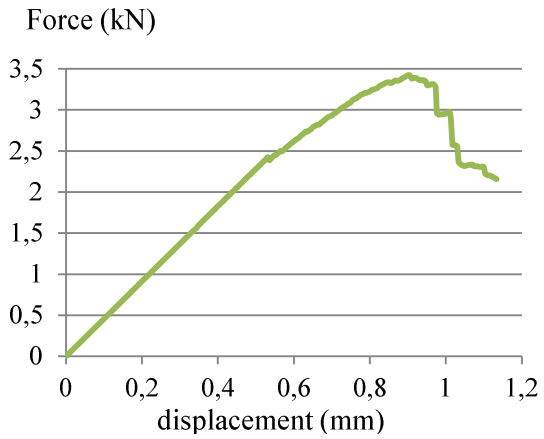

Figure 12. Typical experimental force/displacement curve

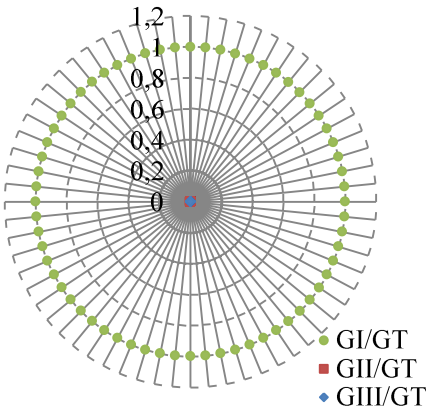

Figure 13. Evolution of normalized G_I, G_{II}, G_{III} along the circular crack tip in ERC-I test

5.Conclusions

The results show that ERC-specimen is quite promising to realize pure mode I, mode II and mode III delamination tests.
(1)Pure mode I, II and III delamination can be realized by using ERC specimen.
(2)The evolution of the strain energy release rate along the crack tip is fairly uniform with a negligible variation. Therefore, it's meaningful to look for a closed-form expressions for these tests.
(3)The geometries are the same for mode I, mode II and mode III delamination tests so the deviation caused by geometry changes is avoided.
(4)Mixed mode tests can be realized by using ERC specimen. For example, mixed mode I+II delamination can be realized under tensile load when stacking sequence is not symmetrical relative to the crack plan. Mixed mode I+III can be realized under a torsion and tensile load at the same time. Mixed mode II+III can be realized when the specimen point deviates from axial centre under torsion load.

Acknowledgments

This work is supported in part by the scholarship from China Scholarship Council (CSC).

References

[1]Becht G., Gillespie Jr., J.W., Design and analysis of the crack rail shear specimen for mode III interlaminar fracture. *Composites Science and Technology,* 1988;31, 143–157.
[2]Donaldson S.L., Mode III intelaminar fracture characterization of composite materials. *Composites Science and Technology,* 1988;32,225–249.
[3]Lee S.M., An edge crack torsion method for mode III delamination fracture testing. *J Compos Technol Res,* 1993;15(3):193–201.
[4]Gong X.J., Hurez A., Ge Y.Y., Peng L.L., De Luycker E., Edge Ring Crack Torsion (ERCT) test for pure mode III toughness. *Proceedings of Journées Nationales sur les Composites (JNC/19), Lyon, France, June 29–July 1; 2015.*
[5]E.F. Rybicki, M.F. Kanninen. A finite element calculation of stress intensity factors by a modified crack closure integral. Eng Fract Mech 1977;9:931-8.
[6]R. Krueger. The virtual crack closure technique: history, approach and applications. NASA/CR-2002-211628.